13, 4576 (1976).
[11]J. Duran, Y. Merle d'Aubigné, and R. Romestain, J. Phys. C 5, 2225 (1972).
[12]D. Lemoyne, J. Duran, M. Billardon, and Le Si Dang, Phys. Rev. B 14, 747 (1976).
[13]M. D. Sturge, in *Solid State Phyiscs*, edited by H. Ehrenreich, F. Seitz, and D. Turnbull (Academic, New York, 1967), Vol. 20; R. Englman, *The Jahn-Teller Effect in Molecules and Crystals* (Interscience, New York, 1972).

Electronic Structures of GaAs-$Ga_{1-x}Al_xAs$ Repeated Monolayer Heterostructure

Ed Caruthers* and P. J. Lin-Chung
U. S. Naval Research Laboratory, Washington, D. C. 20375
(Received 4 April 1977)

We present the first pseudopotential calculation of the fundamental band gaps for heterostructures consisting of alternating monolayers of GaAs and $Ga_{1-x}Al_xAs$ ($0 \leq x \leq 1$). Significant differences are found between the GaAs-AlAs gaps and those of the $Ga_{0.5}Al_{0.5}As$ random alloy. The imaginary part of the dielectric function has been calculated for GaAs-AlAs and appears consistent with the experimentally reported optical absorption edge.

With molecular beam epitaxial techniques (MBE) it is possible to grow repeated heterostructures made up of very thin layers of semiconducting materials.[1,2] One of the most interesting features of these materials is that they add a periodic potential along the heterostructure axis to the usual lattice periodic potential. By changing the layers' composition and thickness basically new devices are produced with energy bands and electronic properties artificially varied over wider limits than exist in "naturally occurring materials." Recently Gossard and co-workers have reported producing the GaAs-AlAs monolayer heterostructure.[3] This requires depositing alternate single monolayers of Ga, As, Al, and As on the (001) GaAss substrate. In this Letter we report the first theoretical study of the energy spectrum of the monolayer material using the semi-empirical pseudopotential method. The motivation for this study is twofold. First, unlike heterostructures whose layers are between a few tens and a few hundreds of angstroms thick and whose potential in the z direction can be represented by a series of rectangular wells capable of trapping carriers in two-dimensional quantum states, the properties of much thinner heterostructures cannot be calculated from the effective-mass approximation in the Kronig-Penney model. As the layers become thinner the quantum states extend through the barriers and couple,[4] eventually losing all two-dimensional character. Thus in the monolayer case, a three-dimensional band structure calculation is needed; a pseudopotential method is capable of serving this purpose well. Second, because self-diffusion constants usually quoted for high quality III-V crystals are from 10^{-11} to 10^{-14} cm^2/sec,[5] it might be expected that such thin layers would completely blend together producing a $Ga_{2-x}Al_xAs_2$ random alloy. However, Dingle has inferred $D < 10^{-22}$ cm^2/sec for multilayer heterostructures grown at 600°C.[6] But this implies similarly small diffusion in the monolayer structure only if the small D results from the MBE method and not from the multilayer structure itself. This prompted us to calculate the composition dependence of the band structures of both the repeated monolayer material and the usual random alloy. We have also calculated ϵ_2 for GaAs-AlAs in order to provide a basis for comparison with optical experiments. Full energy bands and details of the calculation will appear in a later paper.

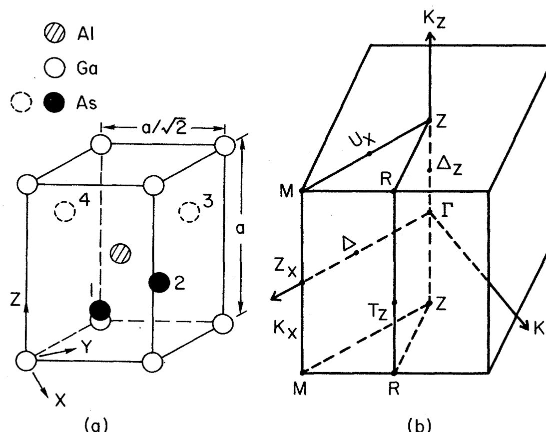

FIG. 1. (a) Tetragonal unit cell of GaAs-AlAs monolayer. (b) Brillouin zone of the monolayer structures.

The GaAs-AlAs monolayer structure shown in Fig. 1(a) has a tetragonal unit cell. It contains four basis atoms and has D_{2d}^1 space group symmetry. The Brillouin zone (BZ) shown in Fig. 1(b) is one-half the size of the zinc-blende BZ.

We express the GaAs-$Ga_{1-x}Al_xAs$ crystal pseudopotential in terms of atomic form factors $V_{Ga}(G)$, $V_{Al}(G)$, and $V_{As}(G)$:

$$V(r)=\sum_{\vec{G}} \exp(-i\vec{G}\cdot\vec{r})\{V_{Ga}(G)+[(1-x)V_{Ga}(G)+xV_{Al}(G)]\exp(-i\vec{G}\cdot\vec{\tau}_0)+V_{As}(G)[\exp(-i\vec{G}\cdot\vec{\tau}_1)+\exp(-i\vec{G}+\vec{\tau}_3)]\}, \quad (1)$$

where $\vec{\tau}_0=(0,a/2,a/2)$, $\vec{\tau}_1=(a/4,a/4,a/4)$, $\vec{\tau}_3=(a/4,3a/4,3a/4)$, the $\vec{G}$'s are the reciprocal lattice vectors, and $a=5.64$ Å, the GaAs lattice constant. A detailed comparison of the atomic form factors to previous zinc-blende semiconductor pseudopotentials will be published later. For the moment it is sufficient to say that they reproduce the fundamental band gap of GaAs ($\Gamma_1^c-\Gamma_{15}^v=1.54$ eV[7]) and of AlAs ($X_1^c-\Gamma_{15}^v=2.238$[8]) to better than 0.03 eV, and the next few higher gaps to better than 0.1 eV. They also give the GaAs L_1^c level below the X_1^c level, in agreement with recent experiment.[9] The pseudo wave functions at 60 points, $\vec{k}$, in the BZ have been expanded in all plane waves of momentum, $\vec{K}_j=\vec{k}+\vec{G}_j$, such that $|\vec{K}_j|\leq 27(2\pi/a)$ (about 190 $\vec{K}$'s at a general point in the BZ), Lowdin's perturbation procedure was used to reduce the order of the secular equation to 100 or less.

The calculated composition dependence of the GaAs-$Ga_{1-x}Al_xAs$ band edges is shown in Fig. 2(a). For comparison we show in Fig. 2(b) the composition dependence of the band edges of the zinc-blende alloy, $Ga_{1-x}Al_xAs$, calculated using the same form factors. The dashed lines in Fig. 2(a) reproduce the $0\leq x\leq\frac{1}{2}$ part of Fig. 2(b) and represent the $Ga_{2-x}Al_xAs_2$ alloy, $0\leq x\leq 1$.

The changed ordering of the Γ_1 and Γ_4 levels with changing x parallels the changed ordering of Γ_1 and X_1 in going from GaAs to AlAs. There is a Z_x conduction band minimum degenerate with Γ_4 at $x=0$, since both derive from the zinc-blende X point. As x increases this level stays always above Γ_4 and we include only a tick mark in Fig. 2(a) to show its position at $x=1$. Because the ordering of the Z_x and Γ_4 minima is determined by potential, not symmetry, an accurate determination of whether the lowest band gap is direct or indirect depends on an accurate potential. Our pseudopotential reproduces GaAs and AlAs bandgaps accurately enough for us to be confident that the lowest GaAs-$Ga_{1-x}Al_xAs$ gap will always be nearly direct. At $x=1$, the conduction band minimum actually lies at $(0,0,\frac{1}{8})2\pi/a$ and is 0.04 eV below Γ_4^c. This difference, however, is very close to the numerical uncertainty of ± 0.02 eV which is present in the computation due to the perturbation procedure.

Figure 2(a) shows an important difference be-

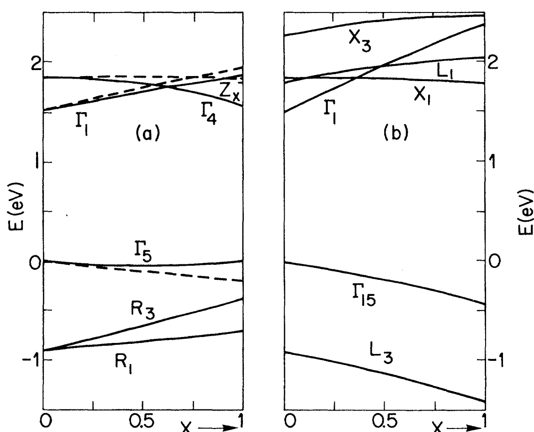

FIG. 2. (a) The compositional dependence of energy levels near the band gap for the GaAs-$Ga_{1-x}Al_xAs$ monolayer structure. (Dashed curves are the $Ga_{2-x}Al_xAs_2$ alloys.) (b) The compositional dependence of energy levels near the band gap for the $Ga_{1-x}Al_xAs$ alloy.

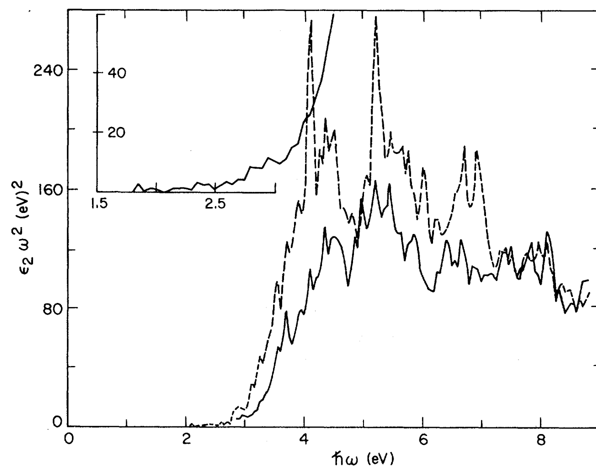

FIG. 3. Optical spectra $\epsilon_2^{\perp}\omega^2$ (solid line) and $\epsilon_2^{\parallel}\omega^2$ (broken line) of $(GaAs)_1$ $(AlAs)_1$. Inset at upper left-hand corner is the enlarged picture of $\epsilon_2^{\perp}\omega^2$ near the absorption edge.

tween the GaAs-AlAs monolayer heterostructure ($x=1$, solid lines) and the $Ga_{0.5}Al_{0.5}As$ alloy ($x=1$, dashed lines). The gap for GaAs-AlAs is nearly direct and is 1.58 eV whereas the minimum band gap for the alloy is indirect and is 2.02 eV. (The calculated alloy gap is in agreement with optical reflectivity measurements.)[10] This large difference can serve to distinguish the true monolayer structure from the alloy. The latter might also arise from the monolayer structure if there were significant interdiffusion of Ga and Al after the monolayer structure was grown.

Unlike the zinc-blende alloy, the (001) and (100) directions in the monolayer structure given in Fig. 1(b) are not equivalent. This inequivalence is introduced by the spatial segregation of Ga an and Al atoms onto alternating planes perpendicular to the (001) direction. Our calculated result for GaAs-AlAs places the conduction band minimum at Z, $(0,0,1)\pi/a$, 0.76 eV below the minimum at the point $(1,0,0)\pi/a$.

In order to provide the basis for a comparison with optical absorption experiments, we extended the calculation over the entire Brillouin zone in sufficient detail to obtain the optical spectrum in the range 0–9 eV. The eigenvalues and oscillator strengths were calculated on a fine mesh in $\frac{1}{8}$ of the BZ given in Fig. 1(b). 12 000 random points were then generated by the Monte Carlo method. Eigenvalues and oscillator strengths at the random points were obtained by a three-dimensional linear interpolation scheme.[11] The imaginary part $\epsilon_2(\omega)$ of the dielectric function so obtained is displayed in Fig. 3. There are strong polarization effects accompanied by alternation of intensities in the $\epsilon_2^{\perp}\omega^2$ and $\epsilon_2^{\parallel}\omega^2$ spectra throughout the energy range. The inset shows details of the $\epsilon_2^{\perp}\omega^2$ spectrum near the absorption edge. There are direct transitions below 2 eV in only a small portion of the BZ. The Γ_5^v-Γ_4^c gap of 1.58 eV is not observable at all since both levels are predominantly p-like and the optical transition matrix element is very small. The edge near 1.87 eV for light polarized perpendicular to the z axis comes from Γ_5^v-Γ_1^c transitions. (The corresponding transition for the alloy case occurs at 2.14 eV.) The 2.08-eV edge for parallel polarized light comes from Γ_4^v-Γ_1^c transitions. (Γ_4^v lies 0.22 eV below Γ_5^v.)

Comparison with experiment is difficult since few samples of GaAs-AlAs monolayer heterostructures have been made, and there was evidence that the one sample reported contained disordered regions along with ordered monolayer domains.[3] However, the weakness of ϵ_2 below 2 eV appears consistent with an optical absorption edge of about 2 eV reported for $(GaAs)_m(AlAs)_n$, $m \gtrsim n \approx 1$. Our present calculation shows, however, that this experiment has not measured the lowest band gap, but, rather, higher transitions. Resonant Raman scattering might better reveal the small gaps.

There have been more experimental observations for multilayer structures than for monolayer structures. Comparisons with multilayer observations are necessarily approximate. But they do indicate that heterostructures made up of thinner and thinner GaAs and $Ga_{1-x}Al_xAs$ layers seem to approach the electronic structures we have calculated. For example, a crude linear extrapolation to the monolayer case from the resonant Raman scattering (RRS) measurements on samples with $x=0.25$ and various layer thicknesses[12] would predict that the first two optical transition thresholds would be about 1.53 and 1.85 eV. Our calculated Γ_5^v-Γ_1^c and Γ_5^v-Γ_4^c for the $x=0.25$ case are 1.65 and 1.86 eV, respectively. As mentioned before, the Γ_5^v-Γ_4^c transition has small oscillator strength and may be seen through strong enhancement of RRS or a two-photon absorption spectrum.

In summary, we have made the first thorough theoretical investigation of the electronic structure of MBE-fabricated monolayer materials. The electronic structures for the monolayer materials are quite different from those of the random alloy systems. This can serve to distinguish these two materials and perhaps can be used in conjunction with detailed experimental optical spectra to determine the Ga,Al diffusion coefficient in the monolayer material. RRS measurements are suggested to locate the fundamental band gap of $(GaAs)_1(AlAs)_1$.

---

*National Research Council–Naval Research Laboratory resident research associate.

[1]L. Esaki and R. Tsu, IBM J. Res. Dev. 14, 61 (1970); A. Y. Cho, J. Vac. Sci. Technol. 8, 531 (1971).

[2]R. Dingle, W. Wiegmann, and C. H. Henry, Phys. Rev. Lett. 33, 827 (1974).

[3]A. C. Gossard, P. M. Petroff, W. Wiegmann, R. Dingle, and A. Savage, Appl. Phys. Lett. 29, 323 (1976).

[4]R. Dingle, A. C. Gossard, and W. Wiegmann, Phys. Rev. Lett. 34, 1327 (1975).

[5]D. L. Kendall, in *Semiconductors and Semimetals*, edited by A. C. Beer and R. K. Willardson (Academic, New York, 1968), Vol. 4, p. 163.

[6]R. Dingle, in Proceedings of the Fourth Annual Conference on the Physics of Compound Semiconductor Interfaces, Princeton, N. J., 8–10 February 1977 (to be published).
[7]M. Cardona, K. L. Shaklee, and F. H. Pollak, Phys. Rev. 154, 696 (1967); D. D. Sell, S. E. Stokowski, R. Dingle, and J. V. Dilorenzo, Phys. Rev. B 7, 4568 (1973).
[8]M. R. Lorenz, R. Chicotka, and G. D. Pettit, Solid State Commun. 8, 693 (1970).
[9]D. E. Aspnes, C. G. Olson, and D. W. Lynch, Phys. Rev. Lett. 37, 766 (1976).
[10]R. Tsu, A. Koma, and L. Esaki, J. Appl. Phys. 46, 842 (1975).
[11]P. J. Lin and J. C. Phillips, Phys. Rev. 147, 469 (1966).
[12]P. Manuel, G. A. Sai-Halasz, L. L. Chang, C. A. Chang, and L. Esaki, Phys. Rev. Lett. 37, 1701 (1976).

Radiative Detection of Single- and Multiple-Pulse Magnetic Resonance of Oriented Radioactive Nuclei

H. R. Foster, P. Cooke, D. H. Chaplin, P. Lynam, and G. V. H. Wilson
Department of Physics, University of New South Wales, Royal Military College, Duntroon, Australian Capital Territory, Australia
(Received 12 April 1977)

Observations by radiative detection of pulse magnetic resonance of oriented ^{60}Co nuclei in iron are reported. Multiple-pulse techniques are used to observe free-induction decays and spin echoes.

Radiative detection of the magnetic resonance of oriented radioactive nuclei by the observation of the effects of a resonant rf field upon the anisotropic distribution of the γ radiation was suggested by Bloembergen and Temmer.[1] The main advantage of radiative detection is that far less nuclei are required as compared with conventional NMR techniques in which the emf induced in the rf coil by the precessing nuclei is detected. Also Shirley[2] pointed out that the effects of resonant fields on the emission of radiation by nuclei are of fundamental interest. Using a model in which the spins of the resonated nuclei are assumed to be evenly distributed around the well-known[3] precessional cone in the Larmor frame, Shirley showed that the dependence of the resonant change in γ-radiation anisotropy upon rf frequency should exhibit structure associated with the various multipole terms in the angular distribution of the emitted radiation.

The first observation of NMR by radiative detection was by Matthias and Holliday[4] using ^{60}Co nuclei oriented by magnetic hyperfine interaction in iron at a low temperature (~ 0.03 K). At the resonant frequency of 165.5 MHz only a small (~ 1%) change in the γ-radiation anisotropy was observed and this was later shown by Templeton and Shirley[5] to be due to the spread (~ 0.1 T) in the hyperfine fields associated with inhomogeneous line broadening. With a single rf frequency ω, only nuclei in the frequency range $\omega \pm \gamma H_1$ will be significantly affected by the rf field, where H_1 is the amplitude of the circularly polarized rf field at the nuclei. With the largest cw rf fields which may be used without intolerable heating of the metallic samples this frequency range is much smaller than the inhomogeneous linewidth. Templeton and Shirley showed that large changes (~ 60%) in the anisotropy may be obtained by employing frequency-modulated rf fields using modulation parameters chosen so that most of the nuclei are resonated at intervals which are short in comparison with the nuclear spin-lattice relaxation time T_1. With use of this technique, accurate measurements of magnetic hyperfine interactions and T_1 values for a wide variety of dilute ferromagnetic alloys have been reported and have recently been reviewed by Stone.[6] In such experiments, each nucleus experiences a series of many fast passages and the effects of coherent spin motion in the rf field are not observable.[7] We recently reported[8] the application of radiative detection to single-pulse experiments using short (~ 2-10 μsec) pulses of high (~ 1 kW) rf power. Values of $\omega_1 = \gamma H_1$ which were comparable with the inhomogeneous width were applied without detectable off-resonant heating. Large signals were observed indicating the feasibility of using fixed-frequency rf pulses. We report here improved results obtained with faster pulse rise times which permit, for the first time, the radiative detection of coherent spin rotations in the